

X-RAY PHOTOELECTRON STUDY OF THE REACTION OF OXYGEN WITH CERIUM*

G PRALINE, B E KOEL, R L HANCE**, H-I LEE and J M WHITE

Department of Chemistry, University of Texas, Austin, Texas 78712 (U S A)

(First received 28 December 1979 in final form 7 April 1980)

ABSTRACT

A clean, polycrystalline Ce-metal surface has been successfully produced by using a sputtering and annealing technique on Ce foil. The chemical species formed upon exposure of Ce to O₂ under UHV conditions at 300 and 120 K have been characterized by XPS. Dissociative chemisorption and reaction occurs to produce a thick layer of Ce₂O₃. Near saturation, a thin layer of CeO₂ is formed over this Ce₂O₃. Two peaks occur in the O(1s) spectra, at BE 529.6 and 530.3 eV, which are assigned to CeO₂ and Ce₂O₃, respectively. An intense Ce(3d) satellite at BE 916.6 eV becomes clearly apparent when Ce(IV) forms. The principal species formed are oxides, and no positive evidence was found for the existence of physisorbed or chemisorbed species.

INTRODUCTION

Cerium is the second, and the most reactive, member of the lanthanide series, and has properties reflecting its 4f orbitals. It is highly electropositive, and has predominantly ionic chemistry due to the low ionization-potential for the removal of the three most weakly bound electrons. The 4f orbitals have small binding-energies, but are localized and well-shielded from the external environment of the Ce atom. Ligand π -bonding is not important in interactions of Ce, and the coordination number is often greater than six. These facts illustrate that cerium differs significantly from the d transition-metals. In addition to the motivation for its study as a consequence of the commercial importance of cerium compounds, cerium metal is a logical choice for the extension of chemisorption studies to more-reactive metals. Also, detailed information on the oxidation of this reactive, 4f-electron

* Supported in part by NSF Grant CHE 77-07827

** Visiting Faculty Member, permanent address Department of Chemistry, Abilene Christian University, Abilene, TX 79601, U S A

metal would be valuable in the development of a detailed theory of the oxidation of metals

Some effects of the exposure of cerium to oxygen have been studied previously, but a clear description has not yet emerged Helms and Spicer [1], using UV photoelectron spectroscopy (UPS), found that an oxide layer forms immediately upon O₂ exposure Using X-ray photoelectron spectroscopy (XPS), Platau et al [2] observed an oxide-derived peak in the Ce(3d) spectrum for very low exposure to O₂ They also found that a protective film of oxide ~10 Å thick was formed Platau and Karlsson [3] have used both XPS and UPS to study the growth and composition of the oxide film Using XPS, Barr [4] examined the passivation layer that forms when Ce is exposed to air and to O₂

A general picture can be obtained from these studies, but a definitive description of the surface species formed is not presented Our purpose was to identify the surface species present during the controlled UHV interaction of O₂ with Ce, from initial to saturation adsorption/reaction, and to compare these results with investigations using O₂ or air at atmospheric pressure Although some differences in passivation may be expected under these conditions, it is important to use UHV to control exposures, to reduce impurities, and to simplify the identification of the surface species

Using XPS, we have studied the interaction of oxygen with clean, polycrystalline cerium foil at 310 and 120 K We are able to clarify the roles of Ce₂O₃ and CeO₂ in the oxidation process at 310 K, while the low-temperature XPS results provide an interesting extension In another paper [5] we present complementary information on the oxidation of cerium by water, and on the chemisorption of water

EXPERIMENTAL

The XPS measurements were made using an ion-pumped Physical Electronics (PHI) Model 548 electron spectrometer which had a base pressure of 1×10^{-10} torr. Mg K α photons ($\hbar\omega = 1253.6$ eV) and a cylindrical-mirror analyzer, operated in the retarding mode at 50-eV pass energy, were used Binding energies are referenced to the Fermi energy (E_F) of clean cerium The work-function of the sample must be added if vacuum reference is desired

Linde extra-dry-grade O₂ was introduced into the analysis chamber by back-filling through a variable leak-valve The exposures were carried out at pressures $< 5 \times 10^{-7}$ torr while pumping the chamber. The total pressure was measured using a Bayard-Alpert ionization gauge, and corrections were made for small increases in the partial pressures of background gases when back-filling

The sample (10 × 10 × 0.25 mm) of 99.9%-pure Ce foil (Ventron, Alfa Products) was first cleaned by mechanical polishing, and then by Ar⁺ ion

bombardment at 5 kV and $150 \mu\text{A cm}^{-2}$. It was necessary to heat the sample to 600 K during sputtering in order to obtain a clean surface (total <0.06 monolayer of impurities, mostly carbon). Complete details of the instrument and the cleaning procedure are given elsewhere [5].

RESULTS

The initial uptake of oxygen is shown in Fig. 1 as a plot of the O(1s) photoelectron-peak area versus O₂ exposure in Langmuirs (L). While Fig. 1 indicates that oxygen uptake has no significant temperature-dependence, the O(1s) and Ce(3d) lineshapes do indicate small differences between the distributions of chemical species at 120 and 300 K. The saturation of the oxygen signal is seen even more clearly from a plot of the O(KVV) Auger peak-to-peak height ($dN(E)/dE$ mode) versus O₂ exposure. These data for exposure at 300 K are shown in Fig. 2, and agree well with the XPS data of Fig. 1. The Auger data also show that there are no sharp discontinuities in the uptake of O₂ by cerium. As indicated below, the oxide thickness exceeds 24 Å for O₂ exposures greater than 20 L, indicating that the saturation shown in Figs. 1 and 2 is not due to cessation of reaction at monolayer coverage, but rather to the oxide thickness becoming greater than the probing depth.

Interesting changes upon oxidation occur in the cerium Auger spectrum. Figure 3a shows the spectrum for clean Ce, while Fig. 3b is for an O₂ exposure of 75 L. The lineshape changes and chemical shifts in the 70–120- and 550–800-eV KE regions are noteworthy. These changes occur smoothly with oxygen exposure, but we have not performed a detailed analysis. However, we note that a previously published spectrum [6] is more characteristic of oxide than of clean Ce.

Helm and Spicer [1] reported that an oxide was formed upon O₂ ex-

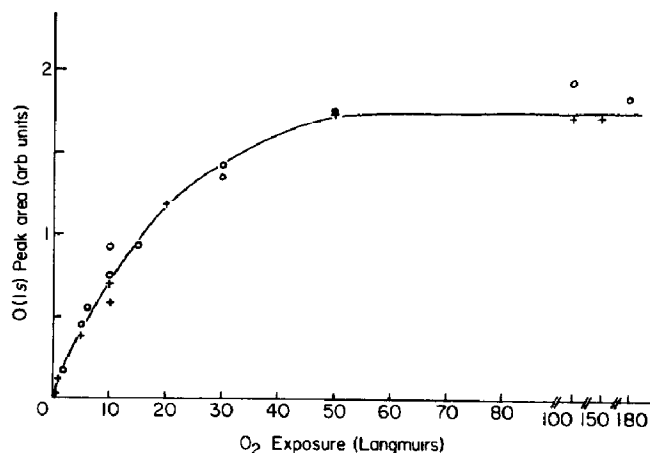


Fig. 1 O(1s) peak-area versus exposure at 300 (○) and 120 K (+) on polycrystalline Ce

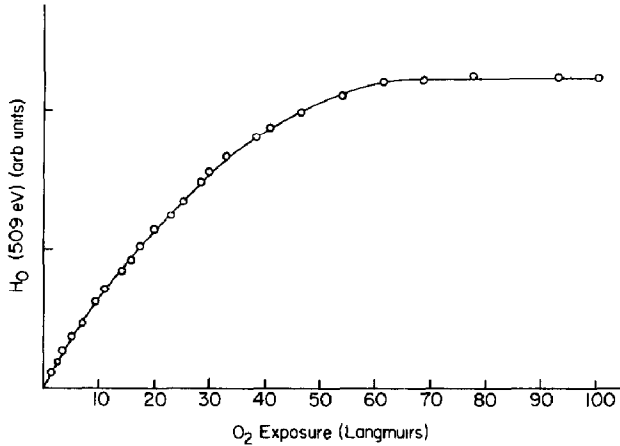


Fig 2 Auger O(KVV) intensity as a function of oxygen exposure at 300 K $P(O_2) = 4.5 \times 10^{-8}$ torr

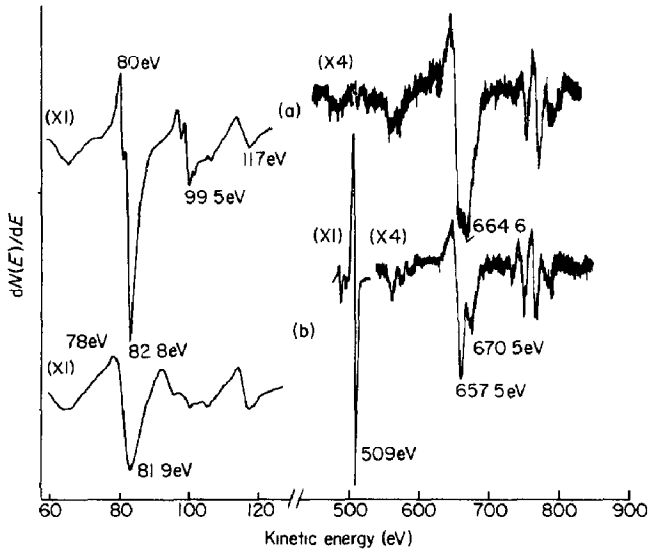


Fig 3 Auger spectra for cerium and oxygen The upper half (a) is for clean Ce, while the lower is for an O_2 exposure of 75 L

posure and that its growth followed a logarithmic relationship, indicating the formation of a semi-protective layer of oxide at low exposures. Slow diffusion of oxygen through this layer at larger exposures gives rise to a passivated surface. The shape of our uptake curve agrees qualitatively with these results. In an XPS study, Platau et al [2] found that the intensity of the O(1s) and of other oxide-related peaks saturates at an O_2 exposure of less than 1000 L, but they did not report an oxygen-uptake curve. In their experiments, a protective oxide layer with an estimated thickness of the order of 10 Å was formed with a large exposure.

The reaction of O_2 with Ce is characterized by two different O(1s) binding energies (BE), 529.6 and 530.3 eV (Fig. 4). Oxygen exposure at 300 K gives initially (0.5-L exposure) a single O(1s) peak at BE 530.3 eV with a full width at half-maximum (FWHM) of 1.9 eV. With further exposure, up to at least 20 L, this peak grows at constant binding-energy. After 30-L exposure to O_2 , the O(1s) spectrum contains essentially a single peak at BE 529.8 eV with an FWHM of 1.9 eV. This peak continues to intensify and shifts by -0.2 eV in going from an exposure of 30 L to saturation. At the highest O_2 exposures, another low-intensity O(1s) peak was sometimes observed at 532.7 eV. We propose that these three peaks are due to CeO_2 , Ce_2O_3 , and $OH(a)$, in order of lowest to highest O(1s) BE. Discussion of each is presented below.

On exposing films of freshly evaporated Ce to O_2 , Platau et al. [2] found

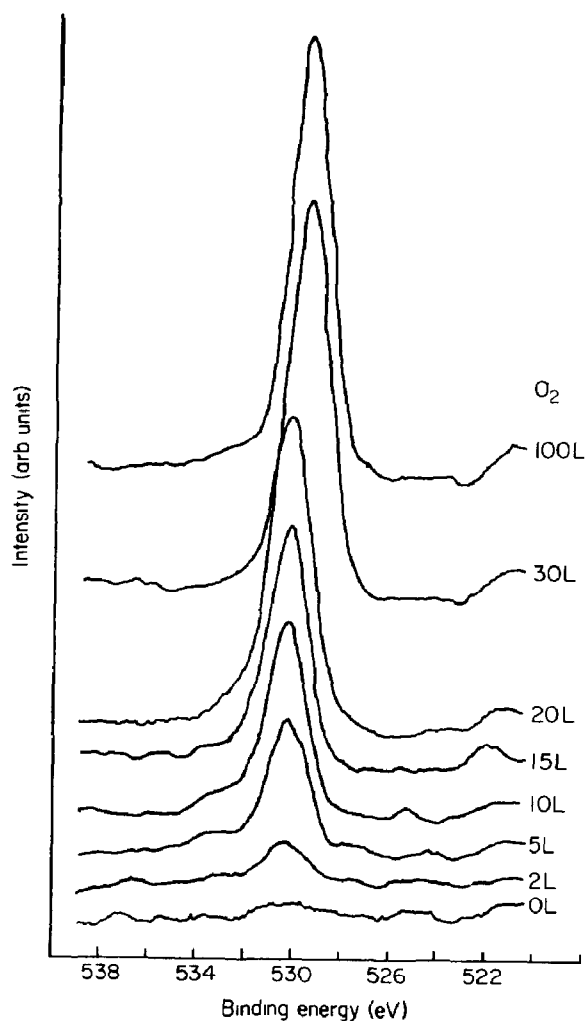


Fig. 4 O(1s) XPS peaks as a function of Ce exposure to O_2 at 300 K

an O(1s) peak at BE 529.9 eV (FWHM 1.8 eV) and a minor peak at BE 532.6 eV. They attributed these features to oxygen in Ce₂O₃ and to physisorbed oxygen, respectively. Their spectra show shifts which are in qualitative agreement with ours: a strong peak at BE > 530 eV for O₂ exposures of less than 40 L, which then shifts to below 530 eV for O₂ exposures exceeding 100 L. They attributed this shift to relaxation and charging differences between the metal and oxide. Our results suggest an alternative interpretation, for the following reasons. Both peaks of Fig. 4 have the same FWHM and both grow at constant binding-energy, suggesting that charging is negligible. In any case, negative sample-charging would cause shifts to *lower* kinetic energy (higher binding energy), contrary to what is observed. Work-function changes and relaxation effects can also be neglected. A change in work-function affects the onset of the electron distribution but has no effect on the observed peak position, since the sample is grounded. Relaxation effects should be greatest when the oxide layer is thin and easily screened by the metal conduction-electrons. Thicker oxide layers should involve less relaxation and higher, rather than lower, binding energies. In the present work, the small shift (-0.2 eV) of the 529.6-eV peak is attributable to a decrease in the relative contribution of Ce₂O₃ as the exposure increases. Between 20- and 30-L exposure to O₂, the O(1s) BE shifts from 530.3 to 529.8 eV. Although we did not investigate this region in detail, the transition occurs over a 5-L exposure interval, the position of which is somewhat sensitive to small amounts of impurities. This shift is attributed to the nucleation and growth of CeO₂ at the surface. On the basis of Ce(3d) spectra (Fig. 5), we must allow some contribution from Ce₂O₃ to the O(1s) signal at 100 L in Fig. 4.

Our observation of a minor O(1s) peak at 532.7 eV agrees with the results of Platau et al. [2]. However, we attribute this peak to OH(a) or to some hydroxyl-containing oxide formed as a result of contamination of the surface by background H₂O, rather than to physisorbed oxygen. Two facts favor this assignment: (1) the intensity of this minor peak varied randomly from experiment to experiment even when O₂ exposure was carried out at 120 K, and (2) exposure to D₂O gave a major O(1s) peak at 532.7 eV [5].

We have repeated these uptake experiments at 120 K and found the same results, except that the O(1s) peak shifts to lower BE at an earlier stage (-0.3 eV by 20-L exposure to O₂). This suggests that, at 120 K, CeO₂ forms at lower exposure. Asymmetry on the high-BE side of this peak (~532 eV) could indicate a small concentration of physisorbed oxygen.

Oxidized cerium, like some other lanthanides, exhibits strong core-level satellite features which are generally attributed to ligand-to-metal charge-transfer transitions [7, 8]. We have focussed on the 3d core level since it is the most intense cerium XPS transition observable and is known to have prominent satellites.

Our Ce(3d) XPS spectra for several exposures to O₂ at 300 K are shown in Fig. 5. Of particular interest are the spectra corresponding to 0-, 20-, 50- and

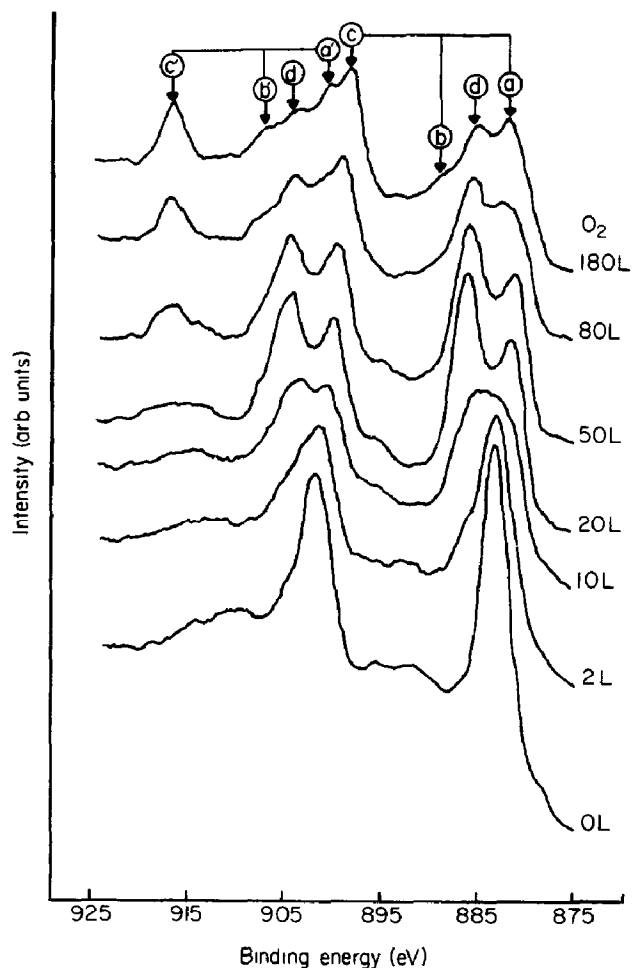


Fig 5 Ce(3d) XPS spectra as a function of O_2 exposure at 300 K. In the uppermost curve, unprimed peaks are assigned to $3d_{5/2}$ and primed to $3d_{3/2}$ transitions

180-L exposure to O_2 , which clearly increase in complexity with exposure. The spectrum of clean cerium is dominated by the $3d_{5/2}$ and $3d_{3/2}$ transitions at BE 883.2 and 901.7 eV, respectively. The spin-orbit splitting of the doublet is 18.5 eV. The measured intensity ratio is 3.02:1, in excellent agreement with the value 3.02:0 expected for a simple spin-orbit doublet. Each of these transitions is accompanied by significant intensity which maximizes ~ 9 eV toward higher BE. This is attributed to $3d$ core-hole- $4f$ electrostatic interactions and is commonly referred to as multiplet splitting [7, 9, 10, 11]. Mg $K\alpha_{3,4}$ X-ray satellites make, at most, a minor contribution to this spectrum.

Referring again to Fig 5, note that a 20-L exposure gives rise to two well-resolved features, separated by 3.7 eV, in both the $3d_{5/2}$ and the $3d_{3/2}$ regions. We attribute these four transitions to Ce_2O_3 , with insignificant

contributions from metallic cerium and CeO_2 . This assignment is made for the following reasons. The peak positions and relative intensities match those for the $\text{Ce}(3d)$ spectrum of Ce(III) species obtained by Barr [4]. Moreover, our spectrum resembles that for Ce(tmhd)_3 , which is distinct from that for Ce(tmhd)_4 [12].*

Oxidation of cerium to Ce_2O_3 gives a $\text{Ce}(3d)$ chemical-shift of 2.6 eV to higher BE, which readily explains the peaks at 885.8 and 904.3 eV. Since metallic cerium should not shift to lower BE, and CeO_2 should be at higher BE than Ce_2O_3 , we assign the peaks at 882.1 and 900.7 eV to shake-down satellites of Ce(III) , perhaps involving $\text{O}(2p) \rightarrow \text{Ce}(4f \text{ or } 5d)$ charge transfer. This assignment has been suggested previously [12]. For exposures between 0 and 20 L, we observed a rapid loss of metal intensity and the steady growth of features attributable to Ce_2O_3 .

Parenthetically, we note that $3d$ XPS spectra of Ce(OH)_3 have been reported [13] which show transitions at 881.7 and 888.0 eV in the $3d_{5/2}$ region. These were assigned as the parent and a charge-transfer shake-up satellite of the Ce(III) species. Due to the marked differences in peak intensities and binding energies from the above Ce(III) results, and the remarkable similarities to Ce(IV) spectra [4, 12], we believe that the spectra of ref. 13 indicate that Ce(IV) species were prevalent at the surface.

Between 20- and 50-L exposure, new features emerge, of which the most recognizable is a new, high-BE peak at 916.6 eV. This feature is characteristic of Ce(IV) , as noted by Barr [4], and in the work of Burroughs et al. [12] on bulk CeO_2 and Ce(tmhd)_4 . The relatively sharp onset of this feature correlates nicely with the shift of the $\text{O}(1s)$ peak discussed above. A significant broadening of the other peaks accompanies the appearance of this feature in the 50-L curve of Fig. 5. We believe this spectrum is a mixture of Ce_2O_3 - and CeO_2 -derived peaks.

With further O_2 exposure (up to 180 L), the high-BE peak intensifies and additional features are resolved in both the $3d_{5/2}$ and $3d_{3/2}$ regions. By comparison with the spectra of Ce(III) and Ce(IV) compounds, we conclude that a 180-L exposure to O_2 at 300 K gives rise to both Ce(III) and Ce(IV) species. Some contribution ($\sim 15\%$) from Ce(III) is required because of the relatively high intensity in the regions a and a' (see Fig. 5). Otherwise, the spectrum is dominated by Ce(IV) .

The development of both the $\text{O}(1s)$ and the $\text{Ce}(3d)$ spectra with controlled exposure to oxygen (Figs. 4 and 5) is consistent with Barr's proposal [4] that oxidation begins with the formation of Ce_2O_3 and terminates with the formation of a thin, passivating layer of CeO_2 . From our data it is not possible to determine the extent to which CeO_2 and Ce_2O_3 are mixed in the outermost layers.

The satellites in the 20-L curve were briefly discussed above. We now turn

* tmhd = 2,2,6,6-tetramethyl-3,5-dionatoheptane

to the assignment of parent and satellite features in the 180-L curve of Fig 5. Each recognizable feature is labelled, unprimed labels denote $3d_{5/2}$ assignments, and primed denote $3d_{3/2}$. The energies of these are assigned (in eV) as follows: $a = 881.8$, $b = 888.1$, $c = 898.0$, $d = 884.8$, $a' = 904.4$, $b' = 906.7$, $c' = 916.6$, and $d' = 903.3$. At the outset, on the basis of the 20-L spectrum and published spectra for Ce(IV) compounds, we recognize that most of these features, while dominated by Ce(IV), do contain unknown contributions from Ce(III) species. Consequently, some peak positions assigned to Ce(IV) may be incorrect. However, excellent agreement with published spectra for CeO₂ [4, 12] is obtained from the peak positions indicated in Fig 5.

One reasonable assignment makes b and b' the parent photoelectron peaks of CeO₂, i.e., roughly $Ce^{4+} \rightarrow Ce^{5+} (3d^{-1})$, with little or no charge transfer. Toward lower BE, the peaks (a, a') and (d, d') are then shake-down satellites involving charge transfer from negatively charged oxygen to the $5d$ and/or $4f$ orbitals of Ce during photoionization. The (a, a') satellites are very intense and lie at 6.3-eV lower BE than the (b, b') pair. The relatively intense peaks labelled c and c' are assigned as shake-up satellites of the parents (b, b') , with $\Delta E = 9.9$ eV. One possibility is a charge-transfer satellite involving $O(2p) \rightarrow Ce(6s)$. These assignments differ from those of Burroughs et al. [12], who argued, on the basis of a point-charge lattice-site model and the instability of Pr(V) compounds, that Ce(IV) compounds should show only shake-down satellites. This argument requires that peaks c and c' be parent peaks and that all other features are satellites. With this assignment, the shift on going from Ce(III) to Ce(IV) becomes 12.3 eV which, based on examination of other metal-oxidation systems, is unusually large. We agree that Ce(IV) shows shake-down charge-transfer satellites, but believe that the equivalent-core Pr(V) argument is not sufficiently strong to be used to eliminate shake-up satellites. With the above assignment, the shift on going from Ce(III) to Ce(IV) is 2.4 eV, which is much more in line with common experience. However, we cannot rule out the possibility that peaks c and c' are parent peaks. Particular care must be exercised here because of the participation of localized f orbitals in screening. Clearly, a theoretical calculation of the energies and intensities of these satellites would be helpful.

We cannot calculate the oxide thickness by standard methods because the metal photoelectron peaks are obscured by the growth of oxide features. After only 20-L exposure to O₂, the intensity of the metal peaks is strongly attenuated. Using a mean free path of 7 Å [14] for the $3d_{5/2}$ photoelectron having KE 370 eV, we find that the oxide overlayer must be at least 24 Å thick after an O₂ exposure of 20 L, and probably becomes substantially thicker with additional exposure. The thickness would be even larger if the mean free path in the oxide were longer than in the metal. Our estimate of the oxide thickness is greater than that of Platau et al. [2] because of differences in the assignments of metal-derived and oxide-derived features.

We have also studied the Ce(3d) region during O₂ exposure at 120 K. As with the O(1s) spectra, we found no significant differences in the binding energies of the peaks. Small differences in the intensity of the satellite at BE 916.6 eV and of associated peaks support the conclusion that a slightly larger amount of CeO₂ is formed at 120 K.

One experiment that does show a temperature effect is the following: Heating a surface to 300 K that has previously been exposed to 50-L O₂ at 120 K causes the loss of CeO₂ features in the spectra. The O(1s) peak shifts from BE 529.6 to 530.3 eV, with a decrease in intensity of ~25%. Also, the Ce(3d) peak at 916.6 eV disappears. The spectrum is similar in appearance to that obtained for 20-L exposure to O₂ at 300 K.

The XPS valence-band region of cerium reveals interesting changes upon oxidation, as shown in Fig. 6. In the range within 10 eV below E_F , the spectrum of clean cerium, curve (c), has a relatively large peak near E_F (maximum at BE 1.3 eV). The intensity near E_F is due to the unresolved

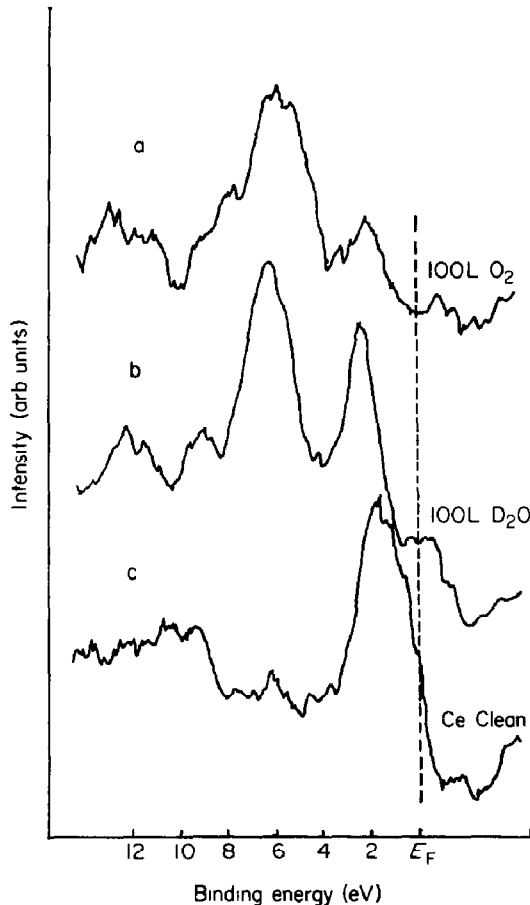


Fig. 6 Spectra of the valence-band region for clean Ce (c), cerium exposed to 100-L D₂O (b), and to 100-L O₂ (a)

combination of the $s-d$ conduction band and the localized $4f$ core-level, and has an FWHM of 3.0 eV. The XPS spectra of the valence-band region of clean cerium have been studied previously [15, 16]. Baer and Busch [15] carried out an approximate deconvolution to obtain a binding energy of 1.8 eV for the $4f$ level, in good agreement with a calculated BE value of 2.0 eV [17]. UPS results are different because the ionization cross-section of the $4f$ level is very small for 20–40-eV photons. However, the location of E_F is confirmed [1].

Curve (a) in Fig. 6 is for 100-L exposure to O_2 at 310 K. There is little overlap of cerium and oxygen features, and interpretation does not require a difference-spectrum. About 16% of the intensity originally present from the clean surface is observed at 2.0 eV, but this intensity is reduced to zero within 1 eV of E_F . The $O(2p)$ peak appears as a broad resonance with a maximum at BE 5.6 eV. The intensity within 4 eV of E_F is severely attenuated, due to the loss of conduction-band and $4f$ electron density in the oxidation by O_2 to Ce(IV). The remaining intensity, which we attribute largely to $4f$ density, is consistent with the formation of a relatively thin layer of CeO_2 on top of a much thicker Ce_2O_3 layer.

At low exposures to O_2 , where the core-level XPS results indicate that mainly Ce_2O_3 is present, a metal contribution to the valence band exists which makes it difficult to interpret the spectra. To obtain a valence-band spectrum of Ce(III) with diminished metal-emission, we have used a D_2O exposure of 100 L, which is known to produce a thick layer of Ce(III) compound and a negligible amount of Ce(IV) [5]. This spectrum is shown as curve (b) in Fig. 6. There is a reduction in the intensity adjacent to E_F , but only small changes occur near BE 2.4 eV. This corresponds to a major reduction of the conduction-band electron density upon oxidation to Ce(III), while the localized $4f$ density is retained. A broad peak due to $O(2p)$ photoelectrons appears at 6.2 eV. The interaction of D_2O with cerium is discussed in detail elsewhere [5]. Helms and Spicer [1] also observed broad, oxygen-derived structure in their UPS valence-band study, which they attributed to emission from oxide bands as opposed to a localized oxide-state.

DISCUSSION

Considerable discussion of our results was included in the previous section, here, we discuss briefly how this work relates to other studies of lanthanides and certain transition metals.

The interaction of O_2 with Ce is very different from that with many of the transition metals, for example Ni [18, 19] and Fe [20]. The most notable difference is the presence, at low adsorption-temperatures, of a high-BE $O(1s)$ transition for most of the transition metals. For Ce, we find no positive evidence for this transition, which is commonly attributed to molecular

oxygen Neither do we find a detectable level of chemisorbed oxygen on Ce Rather, the evidence points to the direct formation of a surface oxide even at 120 K

Compared to the other lanthanides, the behavior of Ce is similar except for the formation of a species characterized by an oxidation number of +4, which is not possible for other lanthanides For example, Lang et al [21] studied the oxidation of ytterbium and found a single O(1s) peak at BE 530.8 ± 0.2 eV, which they attributed to oxide The oxidation of the heavy rare-earth metals, terbium to lutetium, has been studied by Padalia et al [22], using XPS At both 300 and 77 K, the initial uptake of oxygen by clean, evaporated films of these metals was characterized by a single O(1s) peak located at BE 531.0 ± 0.5 eV These authors also found that, with the exception of ytterbium, which has a closed 4f shell in the metallic state, the kinetics of surface oxidation were described by a logarithmic relation between oxide thickness and oxygen exposure They concluded that oxygen adsorption rapidly gives a relatively thick (with respect to the electron mean free paths) oxide film, the growth of which slows down after an exposure of ~ 40 L Our results for Ce show the same kind of behavior except that the surface terminates in a layer rich in Ce(IV)

The conclusion that oxygen reacts with cerium to form Ce(III) and Ce(IV) species is the same as that reached by Barr [4], who focussed on air passivation of Ce Our results, under controlled exposure conditions, give a more detailed picture of the initial stages of oxidation and demonstrate that, even at low exposures and temperatures, oxidation proceeds from Ce(III) to Ce(IV) This lends further empirical support to the notion that many metals tend to be in their highest oxidation states when their surfaces become saturated with oxygen [23] Barr [4] used argon-ion sputtering to determine the depth-profile of oxygen Significantly, our results indicate that no serious artifacts associated with partial reduction were introduced by using this method

As compared to other oxides, we also note that in the case of Ce, an O(1s) chemical-shift is detectable on going from Ce(III) to Ce(IV) Such shifts in the O(1s) BE are not commonly observed, but they have been noted in the oxidation of manganese, for example [24]

Bulk cerium exists in three different phases α , β , and γ [25] At room temperature, the magnetic fcc phase is present As the temperature is lowered, a transformation to β -cerium occurs at ~ 273 K, and another transformation to α -cerium at ~ 110 K The low-temperature α -phase is non-magnetic and is thought to form by the partial transfer of f-electron density into the 5d conduction-band [25] Pollack et al. [16] found little difference between the XPS valence-band and 4d spectra of γ - and α -cerium Our results obtained at 300 and 120 K are consistent with this, but we note that our cleaning procedure involved no annealing after sputtering Thus, we expect that our surfaces have many defects and are not characteristic of a single phase

CONCLUSION

The controlled exposure of clean, polycrystalline cerium to O₂ at 300 or 120 K leads to the rapid development of a relatively thick layer of oxide, with no evidence for chemisorbed oxygen, either molecular or atomic. This oxide develops first as Ce₂O₃, with the metallic-cerium 3*d* XPS peak disappearing after an exposure of 20 L. An exposure of 50 L gives a Ce(3*d*) spectrum with features characteristic of both CeO₂ and Ce₂O₃. In this same exposure-range, a 0.7-eV shift of the O(1*s*) signal to lower BE is noted. At exposures greater than 50 L, the O(1*s*) signal continues to grow slowly at constant BE, while features characteristic of Ce(IV) appear in the Ce(3*d*) region of the XPS spectrum. The reasonability of these assignments is confirmed by comparison with literature spectra for Ce(III) and Ce(IV) compounds. These changes in core-level positions correlate with the loss of conduction-band and *f* electron density in the valence-band region of Ce, and with the increase in O(2*p*) intensity. We conclude that oxidation proceeds by the formation of thick layer of Ce₂O₃ terminated by a thin layer of CeO₂.

The satellites which appear in both Ce(III) and Ce(IV) spectra have been assigned on the basis of chemical shift and reasonable charge-transfer transitions. The latter involve both shake-up and shake-down transitions, provided that our assignment of the parent peaks is correct. These satellites are thought to involve transfer of charge from orbitals derived from O 2*p* to orbitals derived from Ce 4*f*, 5*d*, and 6*s*.

ACKNOWLEDGEMENT

The authors thank Dr J W Rogers, Jr, for helpful discussion of this work.

REFERENCES

- 1 C R Helms and W E Spicer, *Appl Phys Lett*, 21 (1972) 237
- 2 A Platau, L I Johansson, A L Hagstrom, S-E Karlsson and S B M Hagstrom, *Surf Sci*, 63 (1977) 153
- 3 A Platau and S-E Karlsson, *Abstr Rare Earth Res Conf*, 14th, June 1979, p 49
- 4 T L Barr, in N S McIntyre (ed), *ASTM STP 643, ASTM*, 1978, p 83
- 5 B E Koel, G Praline, H-I Lee, J M White and R L Hance, *J Electron Spectrosc Relat Phenom*, 21 (1980) 31 (following paper)
- 6 L E Davis, N C MacDonald, P W Palmberg, G E Riach and R E Weber, *Handbook of Auger Electron Spectroscopy*, Physical Electronics Industries, Eden Prairie, MN, 1976, p 179
- 7 G K Wertheim, R L Cohen, A Rosenzweig and H J Guggenheim, in D A Shirley (ed), *Electron Spectroscopy*, North-Holland, Amsterdam, 1972, p 813
- 8 C K Jørgensen and H Berthou, *Chem Phys Lett*, 13 (1972) 186
- 9 A J Signorelli and R G Hayes, *Phys Rev B*, 8 (1973) 81

- 10 F R McFeely, S P Kowalczyk, L Ley and D A Shirley, *Phys Lett A*, 49 (1974) 301.
- 11 C S Fadley and D A Shirley, *Phys Rev A*, 2 (1970) 1109
- 12 P Burroughs, A Hamnett, A F Orchard and G Thornton, *J Chem Soc , Dalton Trans* , 17 (1976) 1686
- 13 K Tatsumi, M Tsutsui, G W Beall, D F Mullica and W O Milligan, *J Electron Spectrosc Relat Phenom* , 16 (1979) 113
- 14 I Lindau and W E Spicer, *J Electron Spectrosc Relat Phenom* , 3 (1974) 409
- 15 Y Baer and G Busch, *Phys Rev Lett* , 31 (1973) 35
- 16 R A Pollak, S P Kowalczyk and R W Johnson, in R D Parks (ed), *Valence Instabilities and Related Narrow Band Phenomena*, Plenum Press, New York, 1977, p 463
- 17 J F Herbst, D N Lowy and R E Watson, *Phys Rev B*, 6 (1972) 1913
- 18 C R Brundle and A F Carley, *Chem Phys Lett* , 31 (1975) 423
- 19 P R Norton and R L Tapping, *J Chem Soc , Faraday Discuss* , 60 (1975) 71
- 20 J K Gimzewski, B D Padala, S Affrossman, L M Watson and D J Fabian, *Surf Sci* , 62 (1977) 386
- 21 W C Lang, B D Padala, D J Fabian and L M Watson, *J Electron Spectrosc Relat Phenom* , 5 (1974) 207
- 22 B D Padala, J K Gimzewski, S Affrossman, W C Lang, L M Watson and D J Fabian, *Surf Sci* , 61 (1976) 468
- 23 T L Barr, *J Phys Chem* , 82 (1978) 1801
- 24 J C Fuggle, L M Watson, D J Fabian and S Affrossman, *Surf Sci* , 49 (1979) 61
- 25 K A Gschneidier, Jr , in R D Parks (ed), *Valence Instabilities and Related Narrow Band Phenomena*, Plenum Press, New York, 1977, p 89